



Influence of Grating Parameters on the Field Enhancement of an Optical Antenna under Laser Irradiation

Mohammad Reza Mohebbifar^{*,1}, Mehdi Zohrabi²

¹ Department of Physics, Faculty of Science, Malayer University, Malayer, Iran

² Department of Optics and Nanophotonics, Institute of Physics, Kazan Federal University, Kazan, Russia

(Received 11 Sep. 2019; Revised 13 Oct. 2019; Accepted 24 Nov. 2019; Published 15 Dec. 2019)

Abstract: In this study, a new approach for simulation of electric field enhancement of plane wave laser around optical antenna was used to convert free-propagating optical radiation to localized energy. A tapered gold tip design as a novel geometry of optical antenna is introduced and numerically analyzed based on particle swarm optimization (PSO) by solving the Maxwell equations with FDTD simulation Lumerical Software. Five simulation stages of grating parameters to reach the maximum output intensity at the gold tip hot spot were performed with 90° laser incident angle. The optimal values of the grating period “a”, distance of the last circular grating from tip apex “b”, depth of etched grating “T” and duty cycle of grating “D.C” were obtained a=262.2 nm, b=759.5 nm, T=30.1 nm, and D.C.=0.31 respectively. By using these optimal parameters for the gold tapered tip with a cone angle of 30° at room temperature, the maximum output intensity ($|E_{\max}|^2$) at the hot spot was obtained 52.4751.

Keywords: Optical Antenna, Localized Plasmon, Particle Swarm Optimization (PSO), Gold Tip, Surface Plasmon, Field Enhancement

1. INTRODUCTION

The optical antenna is an optical element designed to efficiently transform electromagnetic wave into localized energy, and vice versa [1]. It can increase the optical coupling between electromagnetic wave and the localized excitation of nano-emitters or nano-receivers. In the other words, optical antenna can enhance the interaction between matter and electromagnetic wave in several orders of magnitude and localize the light radiation energy in the sub-wavelength region. Therefore, it is considered as the foundation of many applications in the nano-photonics field [2, 3]. With the help of optical antennas, we can overcome the Abbe limit (diffraction limit) and this, in turn,

* Corresponding author: mmohebbifar@gmail.com

leads to new opportunities in advanced optical spectroscopy and microscopy in the sub-wavelength range. Thanks to these properties, sub-wavelength optical antenna has made the detection of high-frequency spatial features and electronic analyses of vibrational structure of nanoscale objects possible. The metallic nanoparticles with sizes smaller than the wavelength of light show strong dipolar excitations in the form of localized surface plasmon resonances. Actually localized surface plasmon resonances are non-propagating excitations of the conduction electrons of metallic nanoparticles coupled to the electromagnetic field. That is, as soon as the localized plasmon is excited, this results in an increase in the electric field. Properties of localized plasmons significantly depend on the nanoparticles shape, which allows the selective "tune" of the system resonances to effective interaction between matter and light. This subject has potentials for a wide range of novel photonic applications including thermal and chemical sensors [4], near-field microscopy [5, 6], nano-detectors [7], and plasmonic systems [8, 9]. By using an optical antenna, one can concentrate the energy of the laser radiation in a nanometer space. In the recent years, the gold tip is considered as one of the best types of optical antenna. The advantages of this antenna include the break of the limit of diffraction, enhancing the electrical field around the gold tip as a result of the plasmon resonance which is dependent on antenna geometry, and the lightning rod effect [10]. Direct radiations of the tip apex in the Near-field Scanning Optical Microscopy (NSOM) lead to the formation of the background signal and impact on the efficiency of the antenna. To reduce this problem, several studies have been done [11-14]. Berweger *et al.* [11] proposed the concept of adiabatic nanofocusing wherein by decreasing the size of the region in which the electric field enhancement occurs, the background signal partially decreases. In the adiabatic nanofocusing, can excite surface plasmon of the shaft and convey surface plasmon to apex of the tip and convert it into localized plasmon in the apex of tip. In the design of antennas, various geometries have been proposed such as flower-shaped dipole, elliptic dipole nanoantenna by Edgar Briones *et al.* [15], spiral and log-periodic by Mohamed Hussein *et al.* [16]. In [17] J. L. Stokes *et. al.* introduced a tapered-dipole nanoantenna and two geometry were proposed, two-arm and cross-arm dipole antennas with tapered end. Gadalla *et. al.* in [18] was studied the field distribution around nanoantenna and current induced on the surface. In this study, by changing the geometry of the ordinary gold tip and adding circular grating using laser engraving within different time intervals with optimal values, maximum output intensity at the hot spot was achieved. Maxwell equations were solved with FDTD simulation Lumerical Software. In this optimal geometry, a different peak was observed as a result of excitation of surface plasmon of the grating.

2. METHOD

The finite difference time domain (FDTD) or Yee's method is a numerical analysis technique to solve Maxwell's equations with complex geometries [19, 20]. In FDTD, the structural materials and electromagnetic field are characterized on a discrete mesh composed which called Yee cells. This method solves the Maxwell equations in a discrete manner and time step used is related to the mesh size through the stability criterion. The FDTD is a perfect representation of Maxwell's equations in the limit that the mesh spacing goes to zero. The calculated intensities are normalized, with considering the intensity of the incident light. In side illumination, the light is linearly polarized along the tip axis. FDTD is one of the most common computational methods in Photonics and Electromagnetics [21] and many software such as Lumerical software use this method for computing. The FDTD method includes the discretization of Maxwell's equations in both the space and the time domain to find the magnetic and electric fields at different positions and at different time-steps. This method is used to simulate the scattering of electromagnetic waves and radiation from a target of complex shape as well as non-uniform dielectric objects by simply adjusting the size, number and material properties of the Yee cell [22]. The intensity of light is showed by the square of the electric field intensity, which has the same tendency with the light intensity. In order to produce a strong field enhancement at the apex of tip, the electric field of the exciting laser beam needs to be polarized along the tip axis. The effect of material and geometry of tip on the electric field enhancement to find optimum size and material has been reported in various studies [23-26]. The electric field around the optical antenna is calculated and simulated based on Maxwell's equations.

$$E(\mathbf{r}) = E_0 + i\mu_0\mu\omega \int_V \overline{G}(\mathbf{r}, \mathbf{r}') j(\mathbf{r}') dV' \quad (1)$$

$$H(\mathbf{r}) = H_0 + \int_V [\nabla \times \overline{G}(\mathbf{r}, \mathbf{r}')] j(\mathbf{r}') dV' \quad (2)$$

Where E_0 and \overline{G} are the initial electric field and dyadic Green's function for the plane wave laser.

3. SIMULATION RESULTS AND DISCUSSION

The simulations were performed for the gold tip with grating. The geometry of the gold tip is depending on cladding radius, tip radius, and its height. The simulation is Three-dimensional FDTD with a simulation time of 30 femtosecond at room temperature. All boundary conditions are set to Stretched Coordinate PML (SCPML) absorber with standard layers. To accurate study of scattering phenomena in the cone of the tip (hot spot), uses Total-Field Scatter-

Field (TFSF) light source with 400 nm to 1000 nm of wavelength. In order to accurately determined field intensity in hot spot, uses another mesh with 1 nm of size at a hot spot.

In this work the grating was used in order to increase output intensity at hot spot. The characteristics of gratings are improved using Particle Swarm Optimization (PSO) algorithm. This algorithm was first introduced by J. Kennedy and R. Eberhart at the IEEE International Conference on Neural Networks in 1995 [27]. The PSO is a stochastic optimization system based on population, inspired by the social behavior of flocks of birds, and has been used to design and optimize different optical systems [28-31]. In PSO, the potential solutions, which are called particles, placed at random positions, and then move within the parameter search space. The particles are exposed to three forces as they move: (1) personal best position, (2) global best position and (3) particle velocity. The positions of any particle are updated based on the velocity until convergence is achieved [32-38]. The advantages of PSO include Can be simple to implement, Have few parameters to adjust, Able to run parallel computation, Can be robust, Have higher probability and efficiency in finding the global optima, Can converge fast, Do not overlap and mutate, Have short computational time and Can be efficient for solving problems presenting difficulty to find accurate mathematical models. The disadvantages of PSO include Can be difficult to define initial design parameters, Cannot work out the problems of scattering, Can converge prematurely and be trapped into a local minimum especially with complex problems [39]. Due to the capabilities of this optimization method, various researchers have used this method to optimize and design antennas such as El-Toukhy et. al. [40], Jin et. al. [41] and Xu et. al. [42]. Here five simulation steps of grating parameters with the aim of increasing gold tip hot spot intensity was performed. The optical antenna was the grating period “a”, tip-sample distance “b”, depth of etched grating “T” and duty cycle of grating “D.C”. Fig. 1 shows these parameters of the optical antenna. All simulations are based on 90° laser irradiation.

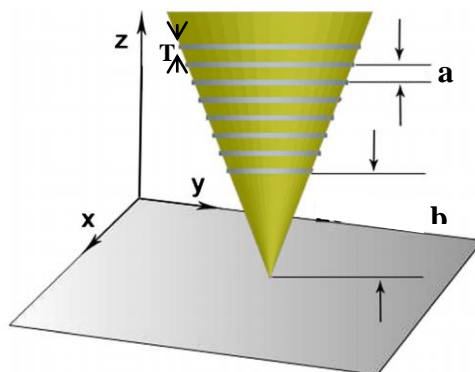


Fig 1. The optical antenna parameters

The basic parameters of the grating are $a=200$ nm, $b=1000$ nm, $T=20$ nm, and duty cycle of 0.31 ($L=60$ nm). The main tip has cladding radius of 520 nm, the cone angle of 30° and tip radius of 10 nm, 3000 nm of height and gold with Johnson and Christy model. The main simulation is configured the same as “without grating” conditions at the cone angle of 30° . At the first step of optimization, parameter “a” is varied from 150 nm to 300 nm. After optimization the optimal value of grating periods was obtained 262.2 nm to achieve 16.8426 of intensity ($|E_{MAX}|^2$) at the hot spot. The simulation is re-done with the optimal value as below. Figs 2 (a) and (b) show the intensity distribution for optimal grating period ($a=262.2$ nm) with 90° laser incident angle in the XY plane and X-axis.

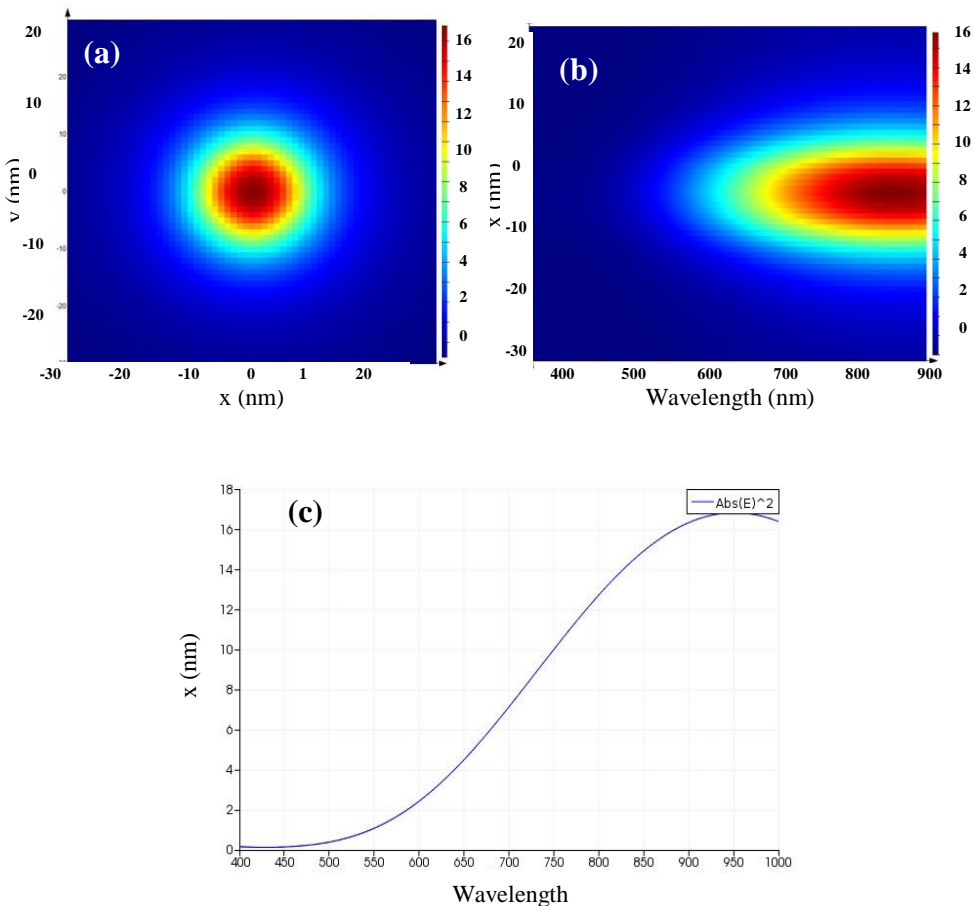


Fig 2. The intensity distribution of output electric field for the optimal grating period ($a=262.2$ nm) in (a) XY plane and (b) X-axis, (c) graph of output electric field in X direction versus wavelength

Fig 2 (c) shows the graph of output electric field in X direction versus wavelength. These figs confirm that there are significant changes in intensity distribution in the plane of X-Y where Z=0 nm.

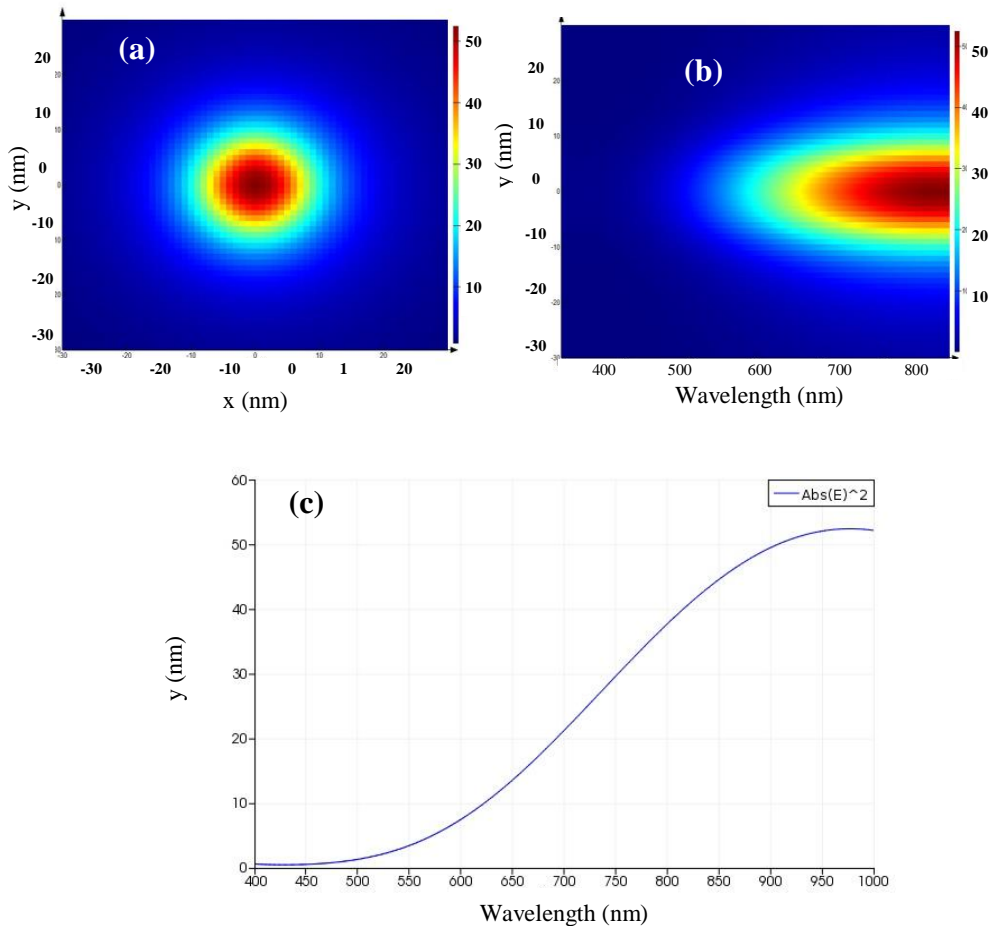


Fig 3. The intensity distribution of output electric field for optimal grating period ($a=262.2$ nm) and the optimal tip-sample distance ($b=759.5$ nm) in (a) XY plane and (b) Y axis, (c) graph of output electric field in Y direction versus wavelength

In the second step of optimization focused on the “b” parameter. By using the optimal parameter of “a” 262.2 nm (fixing this parameter), parameter “b” was optimized from 200 nm to 1200 nm. After optimization, the optimal value of “b” was obtained 759.5 nm with the intensity of 52.4751. Figs 3 (a) and (b) show the intensity distribution for the optimal grating period ($a=262.2$ nm) and

the optimal value of tip-sample distance ($b=759.5$ nm) in XY plane and Y-axis. Fig 3 (c) shows graph of output electric field in Y direction versus wavelength. In the third step of optimization, was concentrated on “a” parameter again to find the best optimal value of grating’s period with fixed “b” parameters. So, used the fixed value of $b=759.5$ nm and find that the best optimal value is same as the first step of optimizations $a=262.2$ nm with a maximum intensity of 52.4751 (Fig 4).

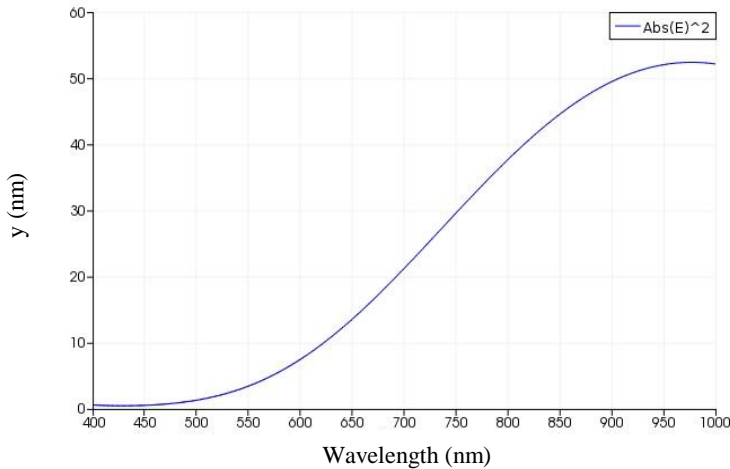


Fig 4. The output electric field in Y direction versus wavelength

In the fourth step of optimization, was motivated on the depth of etched grating (T) with optimal values of “a” and “b” parameters 262.2 nm and 759.5 nm, respectively. The optimal value of $T=30.1$ nm with the intensity of 52.4751 was obtained. Figs 5 (a) and (b) show the intensity distribution for the optimal grating period ($a=262.2$ nm), the optimal value of tip-sample distance ($b=759.5$ nm) and the optimal depth of etched grating ($T=30.1$ nm) in XY plane and Y-axis. Fig 5 (c) shows graph of output electric field in Y direction versus wavelength.

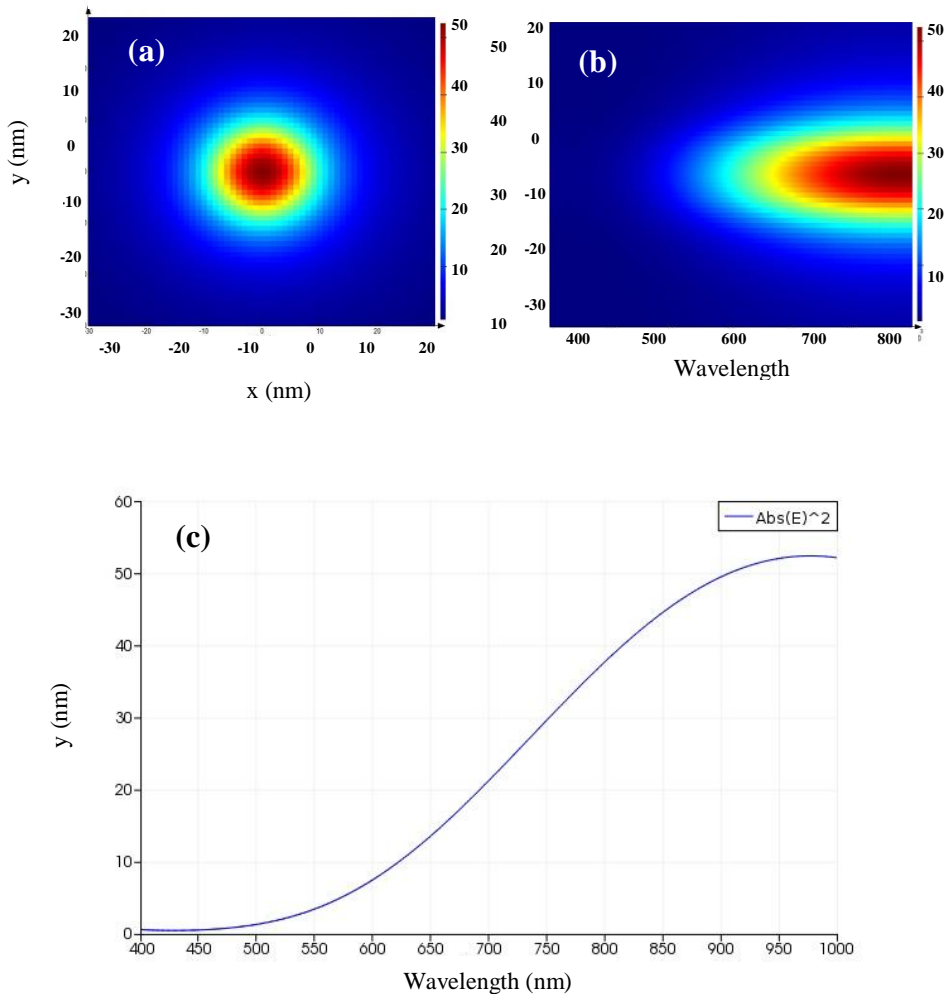


Fig 5. The intensity distribution of output electric field for the optimal grating period ($a=262.2$ nm), optimal the value of tip-sample distance ($b=759.5$ nm) and the optimal depth of etched grating ($T=30.1$ nm) in (a) XY plane and (b) Y-axis, (c) graph of output electric field in Y direction versus wavelength

In order to determine the optimal value of duty cycle (D.C.) at the final step of optimization by using optimal values of $a=262.2$ nm, $b=759.5$ nm, $T=30.1$ nm, optimal value of duty cycle was obtained. The optimal value of duty cycle 0.31 or $L=60$ nm with maximum intensity of 52.4751 was obtained. Figs 6 (a) and (b) show the intensity distribution for optimal grating period ($a=262.2$ nm), optimal value of tip-sample distance ($b=759.5$ nm), optimal depth of etched

grating ($T=30.1$ nm) and optimal value of duty cycle (D.C. =0.31) in XY plane and Y-axis. Fig 6 (c) shows graph of output electric field in Y direction versus wavelength.

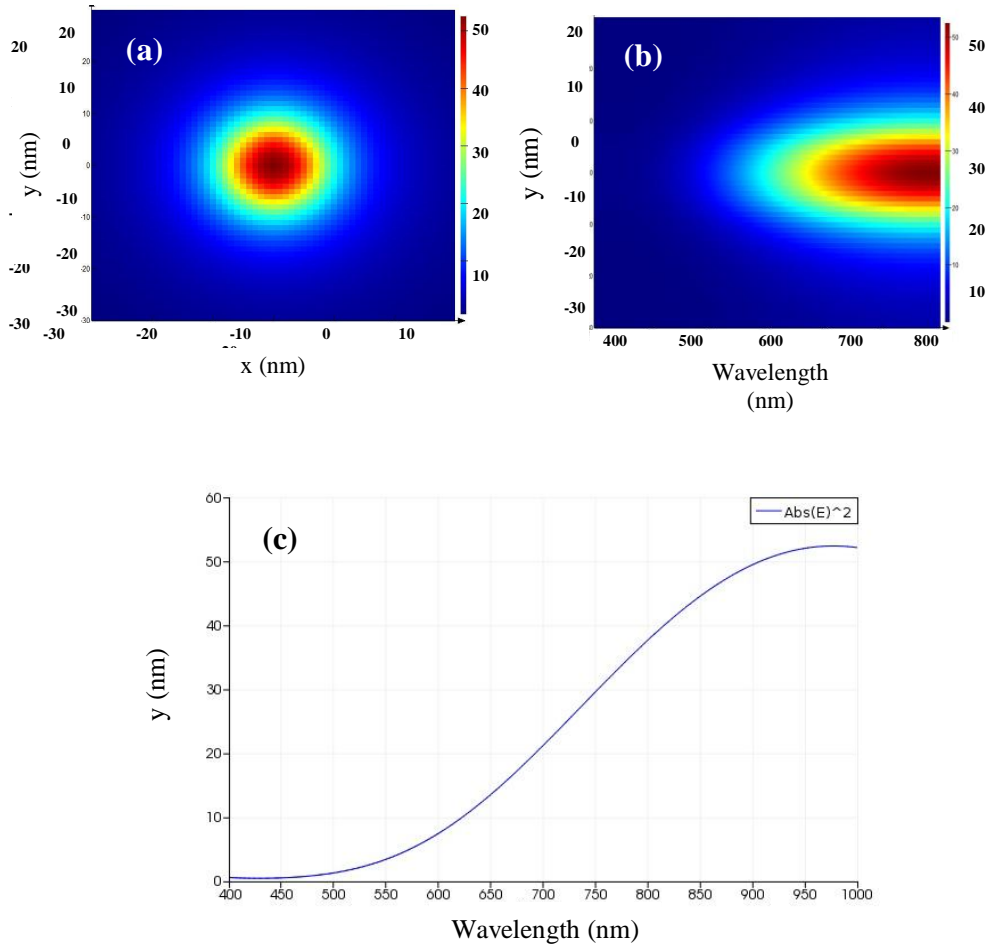


Fig. 6. The intensity distribution of output electric field for optimal grating period ($a=262.2$ nm), optimal value of tip-sample distance ($b=759.5$ nm), optimal depth of etched grating ($T=30.1$ nm) and optimal value of duty cycle (D.C.=0.31) in (a) XY plane and (b) Y axis, (c) graph of output electric field in Y direction versus wavelength

After all optimizations, was simulated structure with all optimal values of $a=262.2$ nm, $b=759.5$ nm, $T=30.1$ nm and D.C.=0.31 to obtain intensity at hot spot in XY plane and ZY plane with mesh size of 0.5 nm and cone angle of 30° (figs 7 and 8).

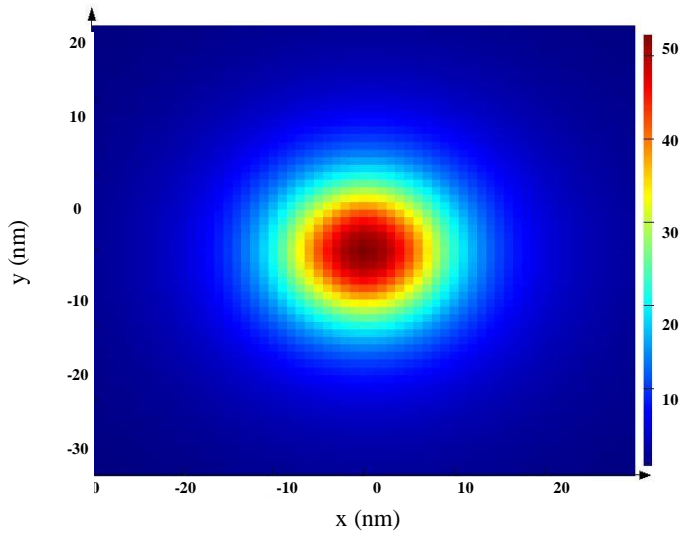


Fig. 7. The intensity distribution of output electric field for all optimal parameters in XY plane

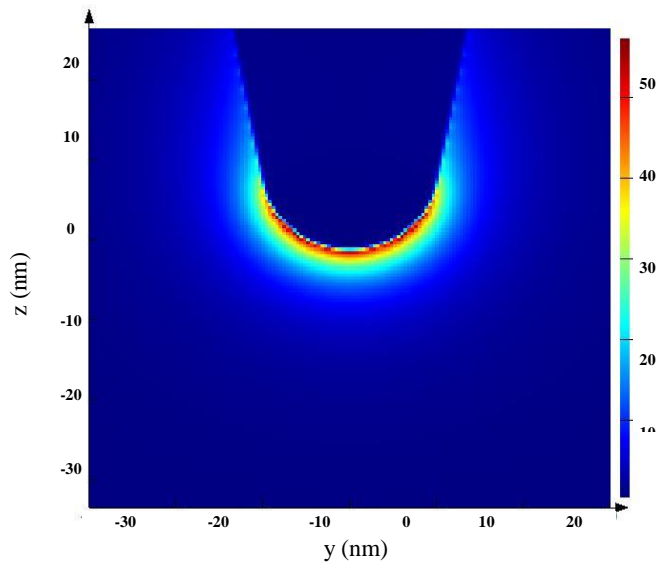


Fig. 8. The intensity distribution of output electric field for proposed grating period in ZY plane

In table 1, all optimization results are summarized.

Table 1. The summary of optimization results

Material	Grating	Optimization of Grating						$ E_{FINAL} ^2$
		Angle	$\frac{a_{1st}[150-300]}{ E_{MAX} ^2}$	$\frac{b[200-1200]}{ E_{MAX} ^2}$	$\frac{a_{2nd}[150-300]}{ E_{MAX} ^2}$	$\frac{T[25-30]}{ E_{MAX} ^2}$	$\frac{D.C.}{ E_{MAX} ^2}$	
Gold	L = 60 T = 20 a = 200 b = 1000	30	$\frac{262.2 \text{ nm}}{16.8426}$	$\frac{759.5 \text{ nm}}{52.4751}$	$\frac{262.2 \text{ nm}}{52.4751}$	$\frac{30.1 \text{ nm}}{52.4751}$	$\frac{60 \text{ nm}}{52.4751}$	52.4751

It is worth noting that in the [43] a novel design of tapered dipole nanoantenna numerically and also in the [44] a nanospiral design of nanoantenna experimentally are showed that selecting the appropriate geometry of the nanoantenna leads to an increase in the electric field around them which in agreement with our results.

4. CONCLUSIONS

In this paper the electric field enhancement of laser around tapered gold tip as the optical antenna with aim of increasing gold tip hot spot intensity was simulated by solving the Maxwell equations. For gold tapered tip with cone angle of 30° at room temperature, the optimal geometry was obtained using PSO algorithm. The optimization results showed that to achieve maximum field intensity at the gold tip hot spot, the optimum values of grating parameters are 262.2 nm grating period, 759.5 nm distance of the last circular grating from tip apex, 30.1 nm depth of etched grating and 0.31 duty cycle of grating. By using these optimal geometry for the gold tapered tip, maximum output intensity at hot spot was obtained 52.4751.

REFERENCES

- [1] L. Novotny, P. Bharadwaj, B. Deutsch, Optical antennas. *Advances in Optics and Photonics* 1(3) (2009, Aug) 438–483.
- [2] Masoud Rezvani, Maryam Fathi Sepahvand, Simulation of Surface Plasmon Excitation in a Plasmonic Nano-Wire Using Surface Integral Equations, *Journal of Optoelectrical Nanostructures*, 1(1) (2016, Mar) 51-64.

- [3] Mohsen Olyaei, Mohammad Bagher Tavakoli, Abbas Mokhtari, Propose, Analysis and Simulation of an All Optical Full Adder Based on Plasmonic Waves using Metal-Insulator-Metal Waveguide Structure, *Journal of Optoelectrical Nanostructures*, 4 (3) (2019, Sep) 95-116.
- [4] Krenz, Peter, Javier Alda, Glenn Boreman, Orthogonal infrared dipole antenna, *Infrared Physics & Technology*, 51(2) (2008, Mar) 340-343.
- [5] Nanfang Yu, Ertugrul Cubukcu, Laurent Diehl, Mikhail A. Belkin, Kenneth B. Crozier, Federico Capasso, David Bour, Scott Corzine, Gloria Höfler, Plasmonic quantum cascade laser antenna, *Applied Physics Letters* 91(17) (2007, Oct) 1-2
- [6] A. Cvitkovic, N. Ocelic, J. Aizpurua, R. Guckenberger, R. Hillenbrand, Infrared imaging of single nanoparticles via strong field enhancement in a scanning nanogap, *Physical review letters*, 97(3) (2006, Sep) 1-4.
- [7] Liang Tang, Sukru Ekin Kocabas, Salman Latif, Ali K. Okyay, Dany-Sebastien Ly-Gagnon, Krishna C. Saraswat, David A. B. Miller, Nanometre-scale germanium photodetector enhanced by a near-infrared dipole antenna, *Nature Photonics*, 2(2) (2008, Jun) 226-229.
- [8] Pelton Matthew, Javier Aizpurua, Garnett Bryant, Metal-nanoparticle plasmonics, *Laser & Photonics Reviews*, 2(3) (2008, Mar) 136-159.
- [9] J. N. Farahani, D. W. Pohl, H.J. Eisler, B. Hecht, Single quantum dot coupled to a scanning optical antenna: a tunable superemitter, *Physical Review Letters*, 95(1), (2005, Jul) 82-90.
- [10] P.F. Liao, A. Wokaun, Lightning rod effect in surface enhanced Raman scattering, *The Journal of Chemical Physics*, 76(1) (1982, Jan) 751-752.
- [11] S. Berweger, J.M. Atkin, R.L. Olmon, M.B. Raschke, Adiabatic tip-plasmon focusing for nano-Raman Spectroscopy, *The Journal of Physical Chemistry Letters*, 24(1) (2010, Feb) 3427-3432.
- [12] Höppener, Christiane, Ryan Beams, Lukas Novotny, Background suppression in near-field optical imaging, *Nano letters*, 1(2) (2009, Mar) 903-908.
- [13] M.R. Mohebbifar, Optical force near the laser illuminated tapered tip, *Belgorod State University Scientific Bulletin*, 51(1) (2019, Mar) 115-120.
- [14] Mehdi Zohrabi, Mohammad Reza Mohebbifar, Electric field enhancement around gold tip optical antenna, *Plasmonics*, 10 (4) (2015, Dec) 887-892.

- [15] E. Briones, J. Alda, F. J. González, Conversion efficiency of broad-band rectennas for solar energy harvesting applications, *Optics Express*, 21(2) (2013, Sep) 412-418.
- [16] M. Hussein, N. F. Fahmy Areed, M. F. O. Hameed, S. S. Obayya, Design of flower-shaped dipole nano-antenna for energy harvesting, *Optoelectronics IET*, 8(1), (2014, Apr) 167-173.
- [17] J. L. Stokes, Y. Yu, Z. H. Yuan, J. R. Pugh, M. Lopez-Garcia, N. Ahmad, Analysis and design of a cross dipole nanoantenna for fluorescence-sensing applications, *Journal of the Optical Society of America B*, 31(3) (2014, May) 302-310.
- [18] M. N. Gadalla, M. Abdel-Rahman, and A. Shamim, Design, optimization and fabrication of a 28.3 THz nano-rectenna for infrared detection and rectification, *Scientific Reports*, 4(6) (2014, Dec) 4270.
- [19] A. Taflove, S. C. Hagness, *Computational Electrodynamics: the Finite - Difference Time - Domain Method*, 3th ed., Artech House press, 2005, 25-45.
- [20] B. C. Galarreta, I. Rugar, A. Young, and F. Lagugn´e-Labarthe. Mapping hot-spots in hexagonal arrays of metallic nanotriangles with azobenzene polymer thin films, *The Journal of Physical Chemistry C*, 115(31) (2011, Oct) 15318–15323.
- [21] L. Novotny, Optical antennas tuned to pitch, *Nature*, 455(8) (2008, Oct), 879-882.
- [22] H.G. Frey, S. Witt, K. Felderer, R. Guckenberger, High-resolution imaging of single fluorescent molecules with the optical near-field of a metal tip, *Physical review letters*, 93(20), (2004, Dec) 200801.
- [23] J.M. Gerton, L.A. Wade, G.A. Lessard, Z. Ma, S.R. Quake, Tip-enhanced fluorescence microscopy at 10 nanometer resolution, *Physical review letters*, 93(18) (2004, Oct) 180801.
- [24] Martin, Y. C., Hamann, H. F., Wickramasinghe, H. K., Strength of the electric field in apertureless near-field optical microscopy, *Journal of Applied Physics*, 89 (1) (2001, Jan) 5774–5778.
- [25] Liming Zhu, Yiheng Yin, Lingling Dai, Yanhui Hu, Jiang Nan, Zheny iZheng, Chen Cai, Weisheng Zhao, Ming Ding, Round-tower plasmonic optical microfiber tip for nanofocusing with a high field enhancement, *Optics Communications*, 453(15) (2019, Dec) 124358.

- [26] James P. Heath, John H. Harding, Derek C. Sinclair, Julian S. Dean, Electric field enhancement in ceramic capacitors due to interface amplitude roughness, *Journal of the European Ceramic Society*, 39(4) (2018, Nov) 1170-1177.
- [27] J. Kennedy, R. Eberhart, Particle Swarm Optimization, *Proceedings of IEEE International Conference on Neural Networks*. 4(1) (1995, Jan) 1942-1948.
- [28] Edgar Briones, Riemann Ruiz-Cruz, Joel Briones, Natalia Gonzalez, Jorge Simon, Mayela Arreola, Gregorio Alvarez-Alvarez, Particle swarm optimization of nanoantenna-based infrared detectors., *Optics express* 26(22) (2018, Mar) 28484-28496.
- [29] Eduardo Fontana, Thickness optimization of metal films for the development of surface-plasmon-based sensors for nonabsorbing media, 45(29) (2006, Oct) 7632-7642.
- [30] David Furman, Benny Carmeli, Yehuda Zeiri, Ronnie Kosloff, Enhanced particle swarm optimization algorithm: Efficient training of reaxff reactive force fields, *Journal of chemical theory and computation* 14(6) (2018, May) 3100-3112.
- [31] Rogelio Rodríguez-Oliveros, Ramón Paniagua-Domínguez, José A. Sánchez-Gil, Demetrio Macías, Plasmon spectroscopy: Theoretical and numerical calculations, and optimization techniques, *Nanospectroscopy* 1(1) (2016, Feb) 67–96.
- [32] Y. Shi, R.C. Eberhart, A modified particle swarm optimizer, Presented at *Proceedings of IEEE International Conference on Evolutionary Computation* (1998, May) 69–73.
- [33] J. Kennedy, The particle swarm: social adaptation of knowledge, Presented at *Proceedings of IEEE International Conference on Evolutionary Computation* (1997, May) 303–308.
- [34] J. Kennedy, R. C. Eberhart, *Swarm Intelligence*, 1st edition, Morgan Kaufmann press, 2001, 1-55.
- [35] R. Poli, An analysis of publications on particle swarm optimisation applications, Technical Report CSM-469, Department of Computer Science, University of Essex, UK. (2007, Apr)
- [36] R. Poli, Analysis of the publications on the applications of particle swarm optimisation, *Journal of Artificial Evolution and Applications*, 24(5) (2008, Sep) 1–10.

- [37] M. R. Bonyadi, Z. Michalewicz, *Evolutionary Computation*. 25 (1) (2017, Feb) 1–54.
- [38] Y. Zhang, A Comprehensive Survey on Particle Swarm Optimization Algorithm and Its Applications, *Mathematical Problems in Engineering*, 13 (5) (2015, Mar), 931256.
- [39] Zeineb Abdmouleh, Adel Gastli, Lazhar Ben-Brahim, Mohamed Haouari, Nasser Ahmed Al-Emadi, Review of optimization techniques applied for the integration of distributed generation from renewable energy sources, *Renewable Energy* 113 (12) (2017, Dec) 266-280.
- [40] Y. M. El-Toukhy, A. M. Heikal, M. F. O. Hameed, M. M. Abd-Elrazzak, and S. S. A. Obayya, Optimization of nanoantenna for solar energy harvesting based on particle swarm technique, Presented at IEEE/ACES International Conference on Wireless Information Technology and Systems (ICWITS) and Applied Computational Electromagnetics (ACES), (2016, Sep) 1-2.
- [41] N. Jin and Y. Rahmat-Samii, Particle swarm optimization for antenna designs in engineering electromagnetics, *Journal of Artificial Evolution and Applications*, 8(1) (2008, Feb) 1-5.
- [42] S. Xu, Y. Rahmat-Samii, D. Gies, Shaped-reflector antenna designs using particle swarm optimization: An example of a direct-broadcast satellite antenna, *Microwave and Optical Technology Letters*, 48 (2) (2006, Mar) 1341-1347.
- [43] Y. M. El-Toukhy, M. Hussein, M. F. O. Hameed, A. M. Heikal, M. M. Abd-Elrazzak, and S. S. A. Obayya, Optimized tapered dipole nanoantenna as efficient energy harvester, *Optics Express*, 24 (4) (2016, Mar) 1107-1122.
- [44] Huaqiao Zhao, Huotao Gao, Ting Cao and Boya Li, Efficient full-spectrum utilization, reception and conversion of solar energy by broad-band nanospiral antenna, *Optics Express*, 26 (2) (2018, Apr) 178-191.

